MM Science Journal | www.mmscience.eu
ISSN 1803-1269 (Print) | ISSN 1805-0476 (On-line)
Special Issue | TEAM 2024
Transdisciplinary and Emerging Approaches to Multidisciplinary Science
11.9.2024 – 13.9.2024, Ostrava, Czech Republic
DOI: 10.17973/MMSJ.2024_10_2024080

TEAM2024-00020

RESEARCH ABOUT M300 MARAGING STEEL METALLIC POWDER FOR USE IN SLM 3D PRINTING

ABDESSELAM MECHALI[1], MAREK SADILEK[1], IVAN MRKVICA[1], JOSEF HLINKA[2], IBRAHIM JAHAN[3], MAREK PAGAC[1], PREETI GAUTAM[1], JAKUB MESICK[1], JIRI HAJNYS[1], JANA PETRU[1]

[1]Department of Machining Assembly and Engineering Metrology, Faculty of Mechanical Engineering, VSB -Technical University of Ostrava, Ostrava, Czech Republic

[2] Department of Materials Engineering, Faculty of Materials and Technology, VSB-Technical University of Ostrava

[3] Libyan Authority of science research

*Corresponding author; e-mail: Abdesselam.mechali.st@vsb.cz

Abstract
A growing number of steel components are being fabricated by 3D metal printing. Using metallic powder as the material fed into the laser is selective laser melting (SLM), one of the most popular and precise techniques. The main focus of this article is the investigation that Renishaw conducted on the powder that was supplied. The powder is made using the gas atomization method, and the powder obtained from the SLM process is then examined. The powder's morphology is analysed using scanning electron microscopy (SEM). The particles were seen to have a spherical shape, with a notable number of satellites attached to their surface. The particle size distribution (PSD) was examined and ranged from 15 to 90 µm. In addition, the porosity exhibited a range of values between 0.03% and 0.12%, with an average value of 0.07%. Additionally, the surface wettability was tested, and it was seen to display a wetting behavior (under 90°) which provided surface energy up to 46.21 $mJ.m^{-2}$.
.

Keywords:
3D printing, porosity, wettability morphology, SLM

1 INTRODUCTION

Recent advancements in 3D printing technology have transformed manufacturing, allowing for the creation of highly functional, lightweight, and complex products across various industries. Among the diverse additive manufacturing methods, Selective Laser Melting (SLM) has gained prominence due to its ability to produce components with superior mechanical properties compared to traditional manufacturing techniques [Mechali et al. 2024, Marsalek et al. 2020]. This technology has opened up new possibilities in design and production, particularly in sectors that require high-performance materials.

SLM's layer-by-layer fabrication approach is especially effective in producing metallic components with exceptional tensile strength and flexibility. This capability is crucial in industries such as aerospace, automotive, and tooling, where structural components must meet rigors standards [Brytan et al. 2022 Fortunato et al. 2018 , Ullah et al. 2020]. The technique allows for the precise control of material properties, which is essential for achieving the desired performance characteristics in these critical applications [Song et al. 2019, Mutua et al. 2018].

Despite its advantages, SLM is a complex process that presents several challenges. The simultaneous involvement of thermal, mechanical, and chemical processes, along with significant metallurgical considerations, makes it difficult to fully understand and predict the behavior of printed components. The presence of solid, liquid, and gaseous states during the SLM process adds to this complexity, making it challenging to develop accurate mathematical models that can simulate the process's outcomes [Hajnys et al. 2020].

A key factor influencing the success of the SLM process is the properties of the metal powder used as the medium. The powder's morphology, particle size distribution, flowability, and porosity are critical in determining the final quality of the printed component [Hajnys et al. 2020]. For example, spherical powder particles, typically produced through gas atomization, offer advantages in terms of fluidity and packing density, which are essential for creating a uniform and high-density powder layer. However,

achieving the optimal particle size and distribution is not without its challenges [Karapatis 2002].

In the specific context of SLM, selecting the appropriate input material is crucial. Maraging steels, which are carbon-free iron-nickel alloys, are particularly well-suited for applications requiring high strength, excellent tensile properties, and superior weldability. These alloys, which include elements such as molybdenum, cobalt and titanium, are commonly used in demanding sectors like aviation, tooling, and military applications [Casalino et al. 2015].

This research specifically examines the behavior of components manufactured from M300 maraging steel utilizing SLM technology. The objective of this study is to examine the morphology of maraging steel powder, then analyse the porosity of the generated components and evaluate the surface wettability of the printed samples. This study aims to enhance our understanding of the interplay between the characteristics of maraging steel and the selective laser melting (SLM) method and how they impact the performance of printed components.

2 MATERIAL AND METHODS

2.1 PROPERTIES OF THE POWDER

Carpenter Technology Corporation supplied the first batch of M300 maraging steel powder. Energy-dispersive X-ray spectroscopy (EDS) verified the nominal chemical composition that was supplied by the manufacturer (Table 1). There are some minor variations, but given the accuracy of both approaches, it is difficult to assess any departure from the nominal composition. Using scanning electron microscopy (SEM), the morphology of M300 maraging steel was examined. Utilizing the MasterSizer3000 particle size analyzer (Malvern Panalytical Ltd., Malvern, UK), the particle size distribution (PSD) was assessed.

Tab. 1: The M300 maraging steel's chemical composition (wt.%).

Element	Ni	Co	Ti	Mo	Si	Fe
Manufacturer	17-19	7-10	0.30-1.20	4.50-5.20	0.08	Bal
EDS analysis	16.80 ± 0.29	9.40 ± 0.17	0.81 ± 0.06	3.70 ± 0.19	0.40 ± 0.09	67.08 ± 0.30

2.2 3D printing and printing parameter

An SLM Renishaw AM500 3D printer was used in order to construct the samples. A laser that has a maximum power rating of 500 W is included in the machinery that makes up the printer. A purity level of 5.0 was achieved by the inert gas that was used, which was argon. 70 µm was focus size. For the purpose of preventing powder oxidation during the setup process and due to the ineffectiveness of the inert gas in removing metal vapors during the printing process, the chamber was continually purged of air and kept at a level that was lower than 1000 parts per million. QuantAM software, version 5.0.0.135, developed by Renishaw and Wotton under Edge in the United Kingdom, was used to set up the system. The samples were printed directly onto the substrate, and there was a need for support materials. Two samples of dimension 20x20x20mm were built for checking porosity sections perpendicular and parallel to the printing plane. Two samples of dimension 43x10x3mm were built for the calculation of the surface wettability in one build, as shown in figure 1.

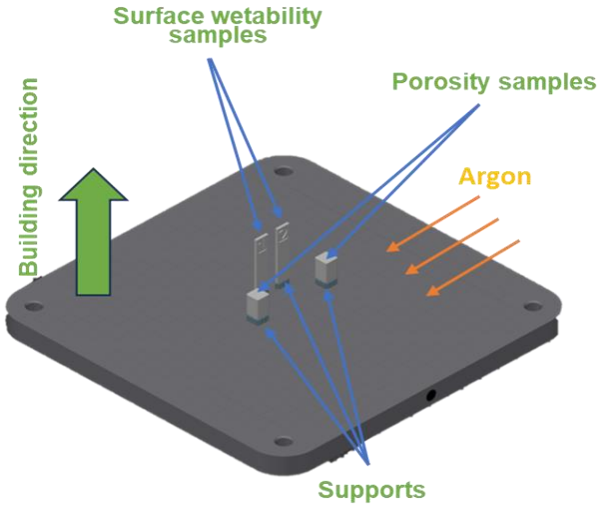

Fig. 1: Schematic graphic depicting the buildup of samples.

Tab. 2: SLM parameters for the manufacturing process.

Parameter	Value
Power of a laser	250 W
Printing strategy	Meander
Spacing between hatches	0.11 mm
Speed of Scanning	650 mm/s
Preheat temperature	Ambient

2.3 Surface wettability:

Before the calculation of surface wettability, we did some surface finishing on specimen number 2. Specimen number 2 underwent tumbling using the OTEC CF1 32EL tumbler for 360 minutes. The device was set to turn at a velocity of 250 revolutions per minute. The tumbling process used three dissimilar materials: ceramic, plastic, and porcelain, while the first specimen was as-built. This analysis aimed to ensure that the post-processed components retained suitable surface characteristics, allowing for a direct comparison with the as-built samples to determine the impact of the post-processing on the material's wettability.

The sessile drop technique was used in order to determine the wettability property of the sample. The SEE system was responsible for determining the surface contact angle, and the Advex Instrument software was responsible for determining the surface energy that is not bound by surrounding materials. The contact angle θ was determined by measuring the tangent to the drop profile at the point where the three phases (liquid, solid, and gas) come into contact with the surface of the sample plane [Hlinka et al. 2020]. 2μL droplets of double-distilled water were applied to the area under examination. The free surface energy of the solid sample is determined Young's Equation (1), where Y_S,Y_{SL}, and Y_L represent the interfacial tensions per unitlength of the solid-vapor, solid-liquid, and liquid-vapor contact line respectively [Hlinka et al. 2020].

$$Y_{sv} - Y_{sl} = Y_{lv} \cos \theta \qquad (1)$$

3. RESULTS AND DISCUSSION:

3.1 Morphology of the powder:

The morphology of powder is an essential feature that impacts the use of metal powder using laser in relation to its flowability and density.

The imaging technique of scanning electron microscopy (SEM) was used in order to examine the powder particles. Images obtained by microscopy of the M300 powder are shown in Figures 2 and 3, which reveal that the particles have a spherical form. As can be observed in figure 2.a, a sizeable proportion of particles have satellites, which are smaller particles, attached to their surface. Satellites are often found on particles (figure3.b). According to the findings of the study of virgin powder, the technique of gas atomization that was used in the production of the powder led to the generation of particles that were not spherical, as shown in figure 2.b. In addition, the satellites are considered to be a defect in the production process [Hajnys et al. 2020].

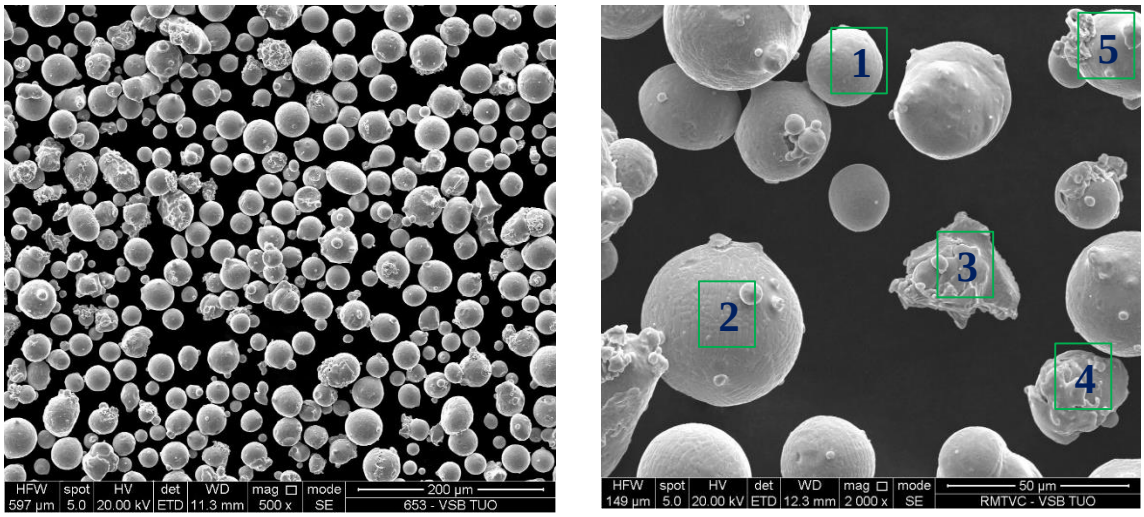

(**a**) (**b**)

*Fig. 2: M300 maraging steel powder (SEM) (**a**) morphology of the particles with 500 x magnification ; (**b**) metallographic with defects with 2000 x magnification (1) spherical particles –(2) spherical with satellites –(3) irregular – (4) splat cap irregular –(5) agglomerated.*

After doing a more in-depth investigation it was found that the particles do not necessarily possess an isometric structure. Alongside the spherical particles as seen in figure 3.a, it is possible to see irregular, elongated, and agglomerated forms in the powders (figure 2.b) . It is primarily believed that the distinctive melting and solidification process that is specific to additive manufacturing (AM) is responsible for this phenomenon. Powders that are smooth and spherical may be difficult to manufacture, despite the fact that they may be chosen for a number of applications in additive manufacturing.

The result is often fairly spherical. It is possible that the morphology of the particles is affected by the thermal conductivity of the molten metal, which is responsible for controlling the rate of cooling that occurs during the formation of particles and the subsequent solidification process.

According to the findings of the examination, the particle sizes were found to fall within the permissible range of 15 to 90µm, as seen in Figure 4. The results for the distribution of particle sizes are summarized in Table 3, which provides a quick summary of the findings. The values of Dv (10), Dv (50), and Dv (90) indicated that they were 23,4 µm, 34,3 µm, and 51,1 µm, respectively. This was viewed as an appropriate distribution for the specified application.

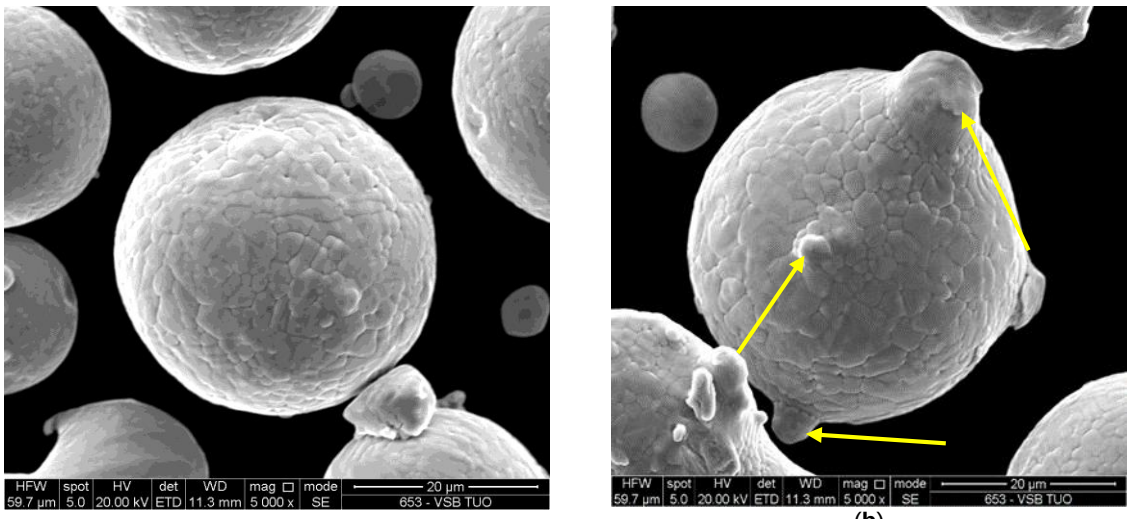

(a) (**b**)

Fig. 3: Morphology of particles (SEM) -a) spherical particles with 5000 x magnification -b) spherical with satellites with 5000 x magnification

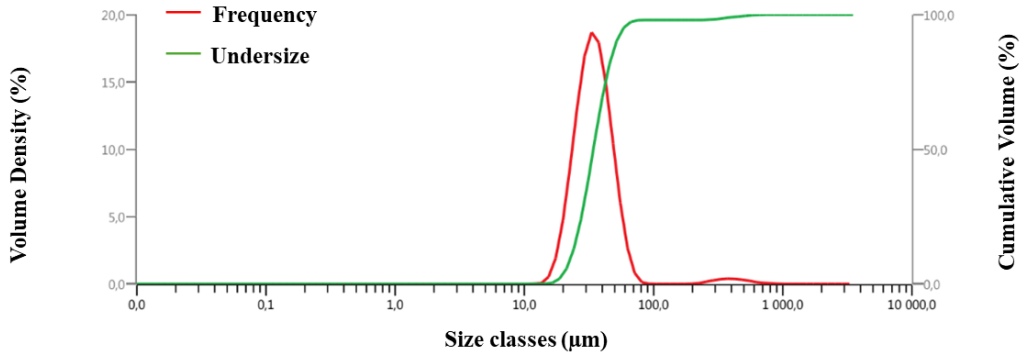

Fig. 4: Frequency (compatible) and Undersize of M300 Maraging steel

Tab. 3: particle size distribution results.

Parameter	Value
Concentration	0,0109 %
Dv (10)	23,4 µm
Dv (50)	34,3 µm
Dv (90)	51,1 µm

3.2 Porosity

Assessing the porosity of the material was accomplished by using the thresholding approach. The overall proportion of black dots that indicated pores was computed after the photos were converted to black and white [Hlinka et al. 2020]. This was done after the photographs were converted. Taking this approach is analogous to the standard that is established by ASTM E1245. It was decided to employ a low magnification in order to lessen the potential impact that may be brought about by the different pore concentrations that were present in the different sample sites. These images were obtained for each sample. These images were shot at a 100 × magnification, and there was no etching present in any of them. Figure 5 displays the typical pictures consisting of samples gathered from each batch. Porosity was calculated five times and averaged in five deferent depths, the measurements of the porosity with the mean porosity values are shown in Table 4, together with the standard derivation of the mean value. The porosity of these samples varied from 0.04% to 0.11% for sections perpendicular to the printing plane and from 0.03% to 0.12% for sections parallel to the printing plane of their entire volume, with a mean value of 0.07% for each section. Comparing our results to the data that was provided in publications [Ronda et al., 2022], where the porosity ranged from 0.12% to 1.12%, we found that our findings on the on the porosity of M300 maraging steel were much lower and considered it appropriate for M300 maraging steel applications. This is related to printing parameters. In general, the mechanical characteristics of printed components, such as tensile strength, Young's module, Poisson ratio, and damping capacity, will decrease as the concentration of porosity increases.

There is a possibility that decreasing the porosity of a material may result in improved mechanical and fatigue performance. This is due to the fact that individual pores have the capability of acting as stress concentrators. The holes were really sealed chambers that do not contain particles of powder; insufficient laser power may result in inadequate melting of the powder particles, causing incomplete fusion either across layers or inside a single layer. This leads to the formation of pores or cavities inside the printed component [Alamri et al. 2022].

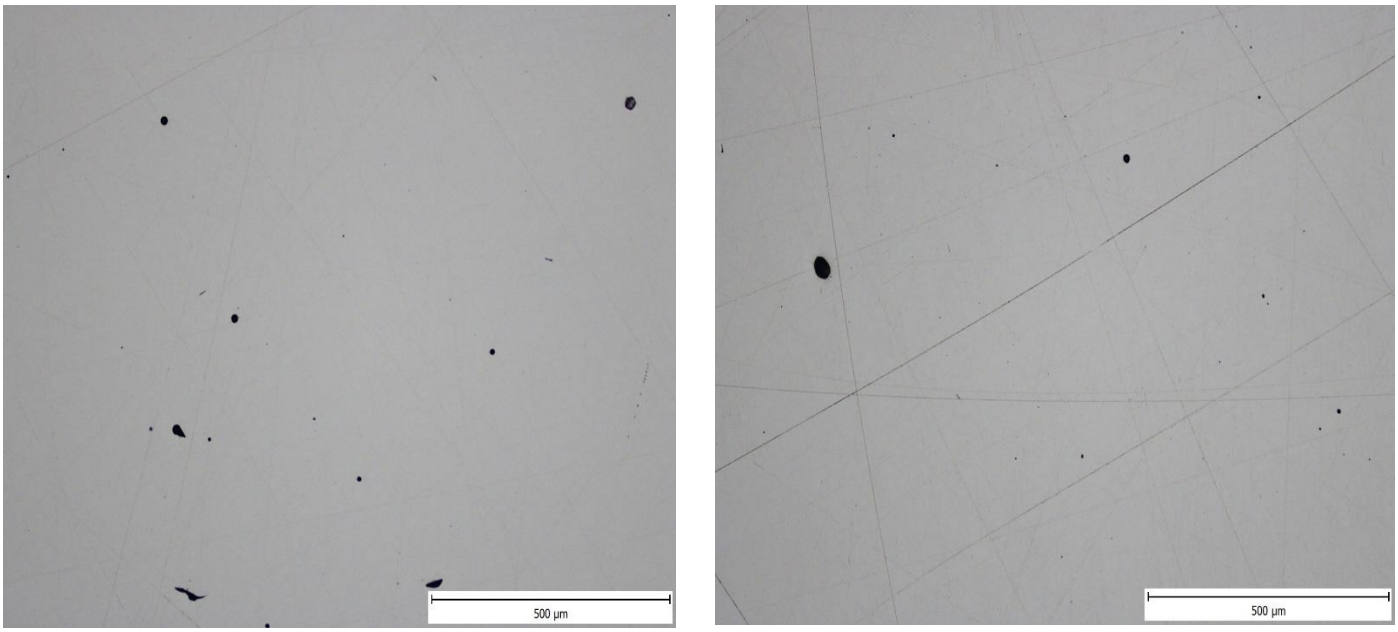

(a) **(b)**

Fig. 5: Macroimages of surfaces of samples used for porosity determination with 100 × magnification (a) sample for section perpendicular to the printing plane (b) sample for section parallel to the printing plane.

Tab. 4: Values of average porosity.

Sample	Measurement 1	Measurement 2	Measurement 3	Measurement 4	Measurement 5	Average porosity (%)
Section perpendicular	0.07	0.08	0.07	0.04	0.11	0.07 ± 0.029
section parallel	0.03	0.07	0.04	0.12	0.09	0.07 ± 0.039

3.3 Surface wettability:

The contact angle measurements were carried out on surfaces that were very precise. This was done to ensure that the findings were not affected by any roughness or surface imperfections that may have been present. In order

to clean each component of the sample in isolation prior to the test being carried out, an ultrasonic bath that contained acetone was used. In order to prevent any potential scratching, the surfaces that were being evaluated were positioned in such a way that they exposed themselves to the upward direction. There was an intentional placing of the droplets outside of the pores that were visible, which may have had an influence on the morphology of the droplets [Hlinka et al. 2020]. During this test, the tumbled sample was compared to as-built sample. Table 5 displays the test results and their corresponding standard deviations, summarizing the average findings. Both Figure 6.a, depicting the as-built sample, and Figure 6.b, depicting the tumbled sample, feature images typical of droplets on the studied surfaces. The tumbling sample's surface wettability is lower than that of the as-built sample, which has the same surface wettability behavior (wetting behavior). The reason for this is that the tumbled sample underwent a rotation. This led to the creation of a unique surface energy value, characterized by a rise in surface energy and a fall in the contact angle. Both the as-built and post-processed samples exhibit wetting behavior when the contact angle is less than 90 degrees, indicating a hydraulic role for both.

Tab. 5: Values of contact angle and calculated surface energy for as-built sample sample and post treated sample.

Sample	Contact Angle (°)	Surface Energy ($mJ.m^{-2}$)	Wetting Behavior
As-built sample	73.27 ± 6.30	40.84	Wetting
Tumbled sample	59.30 ± 4.70	46.21	Wetting

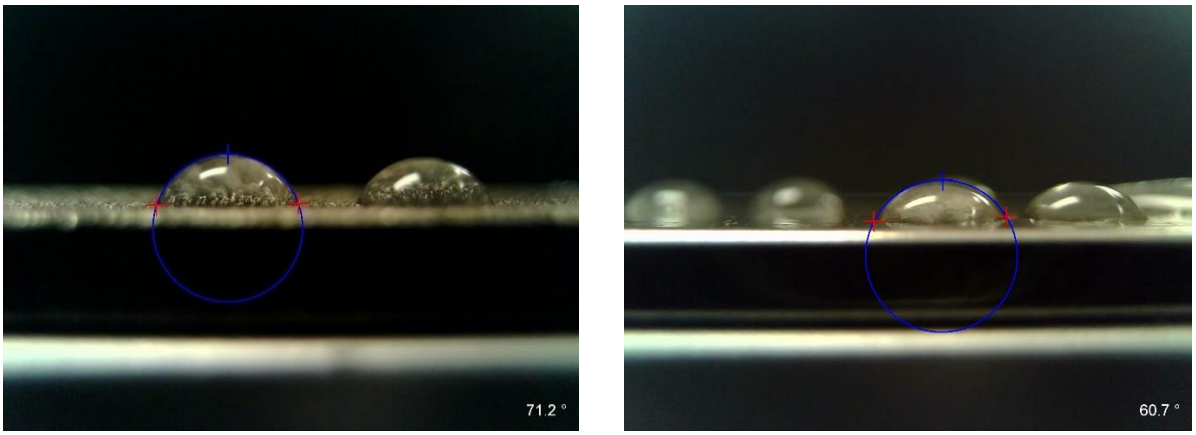

(a) **(b)**

Fig. 6: contact angles with centrifugal tumbling (a) as-built specimen (b) post treated specimen.

4 SUMMARY

The purpose of this study was to investigate the morphology of the virgin M300 maraging steel powder, as well as the porosity and surface wettability of the M300 maraging steel that was printed using SLM. due to Studying powdered metal is an essential foundation for further research in additive technologies. The confirmation of general information about powder morphology, which is mostly influenced by the process used for powder manufacture, has been established, the results of this study can be resumed in the following:

- The particles were discovered to have a spherical shape, with a notable portion of what are known as satellites sticking to the surface of the particles. The analysis of virgin powder indicates that the gas atomization process results in non-ideal spherical form for some particles. Additionally, satellites are seen as a drawback of the manufacturing technique.
- The particle size distribution (PSD) showed that the size of particles varied from 15 to 90µm. This was considered to be the most suited distribution for the given application. The results for Dv (10), Dv (50), and Dv (90) were 23.4 µm, 34.3 µm, and 51.1 µm, respectively.
- The samples exhibited porosities ranging from 0.03% to 0.12% with mean value of 0.07% for both sections parallel and perpendicular.
- Measurements of the contact angles showed that the SLM-printed sample has a wetting behavior (contact angle under 90); however, post-processing improved the surface wettability of the M300-printed material, which led to an improvement in surface energy.

Due to these results, we highly recommend the use of SLM M300 maraging steel for its practical applications due of its

morphology, suitable particles size distribution, low porosity and wetting contact angle which play a hydraulic behavior.

ACKNOWLEDGMENTS

This paper was completed in association with the project Innovative and additive manufacturing technology - new technological solutions for 3D printing of metals and composite materials, reg. no. CZ.02.1.01/0.0/0.0/17_049/0008407 financed by Structural Funds of the European Union. The article has been done in connection with the project Students Grant Competition SP2023/088 „Specific Research of Modern Manufacturing Technologies for Sustainable Economy “financed by the Ministry of Education, Youth and Sports and Faculty of Mechanical Engineering VSB-TUO.

REFERENCES

[Alamri et al. 2022] Alamri, N. M. H., Packianather, M., & Bigot, S. (2022). Predicting the Porosity in Selective Laser Melting Parts Using Hybrid Regression Convolutional Neural Network. *Applied Sciences*, *12*(24), 12571. https://doi.org/10.3390/app122412571

[Brytan et al. 2022] Brytan, Z., Król, M., Benedyk, M., Pakieła, W., Tański, T., Dagnaw, M. J., Snopiński, P., Pagáč, M., & Czech, A. (2022). Microstructural and Mechanical Properties of Novel Co-Free Maraging Steel M789 Prepared by Additive Manufacturing. *Materials*, *15*(5), 1734. https://doi.org/10.3390/ma15051734

[Casalino et al.2015] Casalino, G., Campanelli, S. L., Contuzzi, N., & Ludovico, A. D. (2015). Experimental investigation and statistical optimisation of the selective laser melting process of a maraging steel. *Optics & Laser Technology*, *65*, 151–158. https://doi.org/10.1016/j.optlastec.2014.07.021

[Fortunato et al. 2018] Fortunato, A., Lulaj, A., Melkote, S., Liverani, E., Ascari, A., & Umbrello, D. (2018). Milling of maraging steel components produced by selective laser melting. *The International Journal of Advanced Manufacturing Technology*, *94*(5–8), 1895–1902. https://doi.org/10.1007/s00170-017-0922-9

[Hajnys et al. 2020] Hajnys, J., Pagac, M., Mesicek, J., Petru, J., & Spalek, F. (2020). Research of 316L Metallic Powder for Use in SLM 3D Printing. *Advances in Materials Science*, *20*(1), 5–15. https://doi.org/10.2478/adms-2020-0001

[Hlinka et al. 2020] Hlinka, J., Kraus, M., Hajnys, J., Pagac, M., Petrů, J., Brytan, Z., & Tański, T. (2020). Complex Corrosion Properties of AISI 316L Steel Prepared by 3D Printing Technology for Possible Implant Applications. *Materials*, *13*(7), 1527. https://doi.org/10.3390/ma13071527

[Karapatis 2002] Karapatis P. A. (2002). *Sub-process approach of selective laser sintering*. Ecole Polytechnique federal de Lausanne.

[Mechali et al. 2024] Mechali, A., Mesicek, J., Ma, Q.-P., Hajnys, J., Gautam, P., Blaha, R., Krisak, D., & Petru, J. (2024). ABRASIVE SURFACE TREATMENT OF ALSI10MG PARTS MADE BY L-PBF. MM Science Journal, 2024(1). https://doi.org/10.17973/MMSJ.2024_02_2023134

[Marsalek et al. 2020] Marsalek, P., Sotola, M., Rybansky, D., Repa, V., Halama, R., Fusek, M., & Prokop, J. (2020). Modeling and Testing of Flexible Structures with Selected Planar Patterns Used in Biomedical Applications. *Materials*, *14*(1), 140. https://doi.org/10.3390/ma14010140

[Mutua et al. 2018] Mutua, J., Nakata, S., Onda, T., & Chen, Z.-C. (2018). Optimization of selective laser melting parameters and influence of post heat treatment on microstructure and mechanical properties of maraging steel. *Materials & Design*, *139*, 486–497. https://doi.org/10.1016/j.matdes.2017.11.042

[Ronda et al. 2022] Ronda, N., Grzelak, K., Polański, M., & Dworecka-Wójcik, J. (2022). The Influence of Layer Thickness on the Microstructure and Mechanical Properties of M300 Maraging Steel Additively Manufactured by LENS® Technology. *Materials*, *15*(2), 603. https://doi.org/10.3390/ma15020603

[Song et al. 2019] Song, J., Tang, Q., Feng, Q., Ma, S., Setchi, R., Liu, Y., Han, Q., Fan, X., & Zhang, M. (2019). Effect of heat treatment on microstructure and mechanical behaviours of 18Ni-300 maraging steel manufactured by selective laser melting. *Optics & Laser Technology*, *120*, 105725. https://doi.org/10.1016/j.optlastec.2019.105725

[Ullah et al. 2020] Ullah, R., Akmal, J. S., Laakso, S., & Niemi, E. (2020). Anisotropy of additively manufactured 18Ni-300 maraging steel: Threads and surface characteristics. *Procedia CIRP*, *93*, 68–78. https://doi.org/10.1016/j.procir.2020.04.059

Mechali Abdesselam

VSB-Technical University of Ostrava

Faculty of Mechanical Engineering Department of Machining Assembly and Engineering Metrology

17. listopadu 2172/15, Ostrava, 708 00, Czech Republic

abdesselam.mechali.st@vsb.cz